

# Exploring the Design Space of Adaptive Polymorphism Models through the Production–Regulation Framework

---

## 1. Purpose

---

This note is a model-construction companion to [Lehmann & Mullon, 2025], which established the mathematical conditions for evolutionary branching and coexistence in oligomorphic populations. Here, those conditions are translated into a library of interchangeable biological modules, each representing a distinct causal mechanism grounded in the production–regulation decomposition. Modules are categorized by their primary functional contribution to the three necessary branching conditions: establishing a singular strategy ( $S=0$ ), generating disruptive selection ( $H>0$ ), and providing stabilizing feedback ( $I<0$ ). By systematically combining these building blocks including coupled modules that influence multiple conditions, users can both classify existing models and generate new, testable hypotheses, covering the full design space from well-established cases to novel hybrid scenarios. Crucially, this framework embeds the S-H-I decomposition within the full stability pipeline of the parent theory, adding convergence stability, hyperbolic stability, and qualitative dissimilarity as essential final checks before a constructed scenario can be considered a plausible, stable adaptive polymorphism.

## 2. Rationale: Deconstructing Branching into Functional Requirements

---

This modular approach is justified because the process of evolutionary branching can be deconstructed into three distinct evolutionary functions, each governed by a specific local fitness derivative:

$$S(x) = \partial p / \partial x \mid y=x \text{ selection gradient}$$

Its role is to locate candidate equilibria by defining the mechanism that balances opposing selective forces. It finds the points where directional selection is zero, independent of their stability.

$$H = \partial^2 p / \partial x^2 \mid x=y=x^* \text{ mutant curvature}$$

Its role is to generate disruptive selection by shaping the curvature of the fitness landscape at an equilibrium. It determines whether divergence is locally favored by creating a "fitness valley".

$$I = \partial^2 p / \partial x \partial y \mid x=y=x^* \text{ cross-derivative}$$

Its role is to provide the stabilizing feedback necessary for coexistence. It specifies how the population's state influences selection through frequency-dependent effects, ensuring that diverged strategies can be maintained.

We can categorize the underlying biological mechanisms based on their functional contribution to the branching process. While many mechanisms are "coupled" and contribute to multiple conditions simultaneously, this approach allows us to ask which part of a model is primarily responsible for establishing an equilibrium (the  $S$ -function), generating divergence (the  $H$ -function), or ensuring coexistence (the  $I$ -function).

Why not  $J$ ? The convergence stability criterion  $J = dS/dx \mid x^*$  emerges only after  $S$ ,  $H$ , and  $I$  are specified, it is a diagnostic outcome, not a building block. However, the Jacobian matrix of the full oligomorphic system is the essential tool for analyzing the long-term stability of the resulting polymorphism.

### 3. The Library of Biological Modules

---

The library presented below contains elemental modules, core causal mechanisms from which more complex models can be built. The organizing principle is each module's primary functional contribution. While every mechanism, as part of the total fitness function, will in principle influence all three local fitness derivatives ( $S$ ,  $H$ , and  $I$ ), we classify modules by the evolutionary role in which their effect is strongest and most characteristic. This primary classification is a tool for clarity, not a claim of exclusivity. Many modules will have secondary effects that alter other conditions, sometimes in important ways. For example, a mechanism chosen to establish a singular strategy ( $S=0$ ) might also change curvature ( $H$ ) or frequency-dependence ( $I$ ) in ways that affect stability. We therefore ask first what is the main evolutionary problem this mechanism solves.

***Does it establish a trade-off to create an equilibrium ( $S=0$ )?***

***Does it generate a fitness valley to cause divergence ( $H>0$ )?***

***Does it provide stabilizing feedback to ensure coexistence ( $I<0$ )?***

This functional approach allows us to deconstruct the causal architecture of any model, from simple to complex. However, the  $S$ - $H$ - $I$  classification is necessary but not sufficient. Any assembled scenario must still pass the additional stability tests from the parent framework, including convergence stability, hyperbolic stability, and qualitative dissimilarity, before it can be considered a plausible long-term adaptive polymorphism.

Notation follows Lehmann & Mullon (2025).

### 3.1. Modules that Establish a Singular Strategy (Contribute to S=0)

Causal Pathway	Parameters	Abstract Term	Example Scenario	Paper Example
<b>Phenotype</b> <b>(Production)</b> <b>(z)</b>	$z_1, z_2$ (opposing performance functions)	$z_1(x)$ $-z_2(x)$	A classic life-history trade-off (e.g., seed size vs. seed number) determined solely by intrinsic physiological constraints.	Conceptual example
<b>Phenotype</b> <b>(Regulation)</b> <b>(<math>e_z</math>)</b>	$q$ (regulatory cue), $z_1, z_2$ (performance functions)	$z_1(x; q)$ $-z_2(x; q)$	Regulatory cue shifts phenotypic trade-off (e.g., socially induced morphology).	Resource specialization, where habitat type ( $q$ ) sets the selective context (Sec. 4.3.1)
<b>Payoff</b> <b>(Production)</b> <b>(<math>\pi</math>)</b>	$B$ (benefit function), $C$ (cost function)	$B(x) - C(x)$	Optimal foraging where payoff depends only on an individual's own strategy, without interference from others.	Conceptual example
<b>Payoff</b> <b>(Regulation)</b> <b>(<math>e_\pi</math>)</b>	$m$ (social context parameter)	$\Pi_s(x,y;m)$ $-\Pi_p(x,y;m)$	Public good vs. private contest; a trade-off between social and private payoffs.	Socially mediated interactions where payoff depend on others' actions (Sec. 5.3.2, Appx. C.2.3)
<b>Phenotype</b> <b>(Mixed: Emergent Trade-off)</b> <b>(<math>z, e_z</math>)</b>	$m$ (environmental modulator), $z_1, z_2$ (performance functions)	$z_1(x, m) - z_2(x)$	The trade-off itself emerges from the interaction of production and regulation.	Life-history evolution where dispersal $m$ gives rise to the trade-off between fecundity and survival (Sec. 4.3.2)
<b>Payoff</b> <b>(Regulated Prod.)</b> <b>(<math>\pi, e_\pi</math>)</b>	$N, v$ (regulatory params), $B, C$ (prod. functions)	$B(x, N, v) - C(x)$	A production-based trade-off (B-C) where the benefit $B$ is modulated by social regulation.	The Contest Model, where the benefit of effort is regulated by the number of competitors $N$ (Sec. 5.3.1)

### 3.2. Modules that Generate Disruptive Selection (Contribute to H>0)

Causal Pathway	Parameters	Abstract Term	Example Scenario	Paper Example
<b>Phenotype (Production) (<math>z</math>)</b>	$k$ (strength of selection), $z_{\text{opt}}$ (location of fitness minimum)	$+k [ z(x) - z_{\text{opt}} ]^2$	Generalist disadvantage; intermediate phenotypes are unfit.	Conceptual example
<b>Phenotype (Regulation) (<math>e_z</math>)</b>	$\sigma$ (niche width), $o_i$ (environmental optima)	$\sum_i q_i \cdot W(z(x), o_i, \sigma)$	An individual's performance has convex returns, but only in the context of specific environmental niches.	Fitness landscape in a spatially heterogeneous environment where intermediates are unfit (Sec. 4.3.1)
<b>Payoff (Production) (<math>\pi</math>)</b>	$h$ (acceleration coefficient)	$h x^2$	Purely intrinsic accelerating returns on trait investment.	(Conceptual Example)
<b>Payoff (Regulation) (<math>e_\pi</math>)</b>	$\sigma_p$ (penalty strength), $w$ (conformity width)	$\pi(x) - \sigma_p \cdot \exp[-(x-y)^2/w^2]$	Social penalty for conformity; individuals with average traits are ostracized, creating a fitness valley.	(Conceptual Example)
<b>Payoff (Mixed) (<math>\pi, e_\pi</math>)</b>	$N$ (competitors), $v$ (prize value)	Emergent from $\Pi(a(x), b(y))$	Disruptive selection emerges from the interaction of a production-side non-linear benefit and a regulatory social context.	The Contest Model, where the winner-take-all prize ( $v$ ) and number of competitors ( $N > 2$ ) combine to create $H > 0$ (Sec. 5.3.1)

### 3.3. Modules that Provide Stabilizing Feedback (Contribute to $I < 0$ )

Causal Pathway	Parameters	Abstract Term	Example Scenario	Paper Example
<b>Phenotype (Regulation) (<math>e_z</math>)</b>	$k$ (interference strength)	$-k \cdot z(x) \cdot z(y)$	Interference between similar phenotypes competing for the same resources.	Implicit in models of character displacement and resource competition (Sec. 4.3.1)
<b>Payoff (Regulation) (<math>e\pi</math>)</b>	$i$ (intensity of interference)	$-i \cdot x \cdot y$	Direct interference competition where others' actions reduce the payoff of one's own.	The Contest Model, where competitors $(N - 1) b(y)$ reduce payoff, and the Preference Evolution Model with interference $-\beta b$ (Sec. 5.3.1, 5.3.2)
<b>Fitness (Regulation) (<math>e_\rho</math>)</b>	$T$ (toxicity coefficient)	$\pi(x) / (1 + T \cdot \bar{y})$	Population-level negative feedback, such as toxic byproduct accumulation.	Conceptual example: the paper discusses fitness-level regulation generally
<b>Mixed (Fitness) (<math>\pi, e_\rho</math>)</b>	$s$ (survival), $q$ (environmental frequency)	$[ s + (1 - s) \cdot \pi_1(x) / e_1(y) ] q \cdot [ \dots ]$	Overlapping generations (production) create a “storage effect” when combined with environmental fluctuations (regulation).	The storage effect in temporally fluctuating environments (Sec. 4.4.1)
<b>Mixed (Phenotype) (<math>z, e_z</math>)</b>	$m$ (dispersal), $z_1$ , $z_2$ (life-history traits)	See Eq. (29)	Limited dispersal ( $m$ ) interacts with a fecundity/survival trade-off ( $z_1, z_2$ ), creating kin competition that provides stabilizing feedback.	Emergence of a life-history polymorphism under limited dispersal (Sec. 4.3.2)

## 4. Mixed Scenarios

The 'Mixed' modules presented in the library are merely illustrative examples of a much larger combinatorial space. A primary strength of this framework is its ability to systematically construct hybrid models by combining production and regulating factors across different levels (Phenotype, Payoff, and Fitness). For instance, as discussed below in the "Peacock's Tail" example, a singular point ( $S=0$ ) can be established by balancing a production factor at the phenotype level with a regulating factor at the fitness level. This multi-dimensional design space for novel models is precisely what the framework is intended to map and explore as a hypothesis-generation tool.

### 4.1. An Illustrative Example: The Peacock's Tail

To illustrate how modules from different levels can be combined, we can deconstruct the classic biological problem of a peacock's tail. The evolving trait is tail length,  $x$ . The singular strategy ( $S=0$ ) is established by a mixed-level trade-off. The benefit comes from a phenotype-level production module (a longer tail is intrinsically attractive). This is balanced by a cost from a fitness-level regulation module (a higher average tail length in the population increases conspicuousness and predation risk for everyone).

The disruptive force ( $H>0$ ) is a pure Payoff (Production) module, independent of predation. The fitness returns on tail length are intrinsically non-linear, a small increase from a short tail yields little benefit, but an increase from a medium tail crosses a threshold of female attention, yielding accelerating fitness returns and creating a fitness valley.

The stabilizing feedback ( $I<0$ ) is a pure Payoff (Regulation) module, also independent of predation. The mechanism is interference competition for the best display sites. As one morph becomes too common, individuals with that tail type compete more intensely with each other for limited, high-visibility spots on the lek. This crowding reduces their average mating success, providing a relative advantage to the rarer morph.

This scenario can be captured by a conceptual invasion fitness function where survival is a general cost, and mating success is determined by both intrinsic attractiveness and competition.

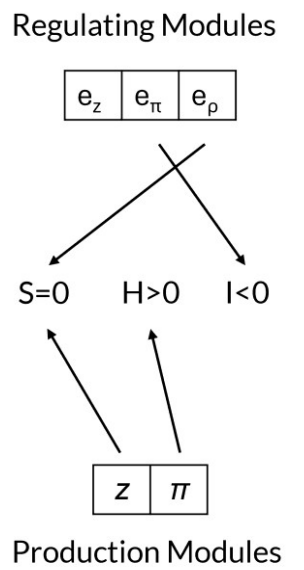
$$\rho(x,y) = [\text{Mate Attraction}(x) - \text{Mating Interference}(x,y)] \times \text{Predation Survival}(y)$$

$$\text{Mate Attraction (Production): } \text{Mate Attraction}(x) = hx^2$$

This term represents the accelerating fitness returns ( $h>0$ ) on tail length. As a production-driven mechanism, it provides the  $H>0$  condition.

$$\text{Mating Interference (Regulation): } \text{Mating Interference}(x,y) = i \cdot p(y) \cdot \delta(x,y)$$

This term describes how the mating success of a male  $x$  is reduced by interference from other males with a similar phenotype  $y$ . As a regulation-driven mechanism, it provides the stabilizing  $I<0$  condition.



## 5. Coupled Scenarios

While the modular framework is a powerful tool for deconstructing the necessary conditions for bifurcation, many realistic biological models are coupled. A system is coupled when a single biological module has pleiotropic effects, exhibiting multiple functional signatures, acting as a "master knob" that affects both the disruptive force and the stabilizing feedback.

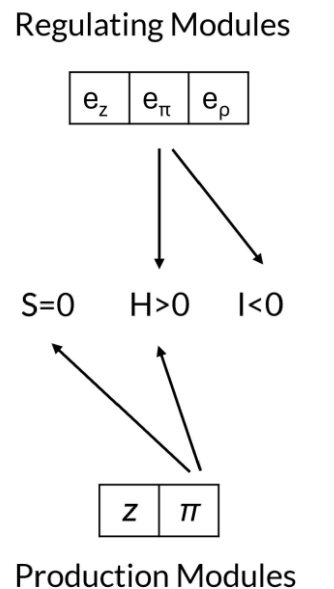
### 5.1. Contest Model

To demonstrate the framework's analytical power, we can deconstruct the Contest Model from the paper (Sec. 5.3.1). In this model, the payoff is a function of competitive effort  $a(x)$ , its intrinsic cost  $C(x)$ , the resource value  $v$ , and the number of competitors  $N$ . The singular strategy ( $S=0$ ) is established by a (Regulated) Production module; the underlying trade-off is between the benefit and cost of effort and then the benefit is modulated by the regulatory parameter  $N$ . Therefore, here production is the primary cause of the trade-off.

The H-Condition is generated by a Mixed (Payoff) module. Disruptive selection is an emergent property of the inseparable interaction between a production factor (the non-linear, "winner-take-all" benefit of the prize  $v$ ) and a regulation factor (the social context of  $N>2$  competitors). Without the winner-take-all prize, there is no potential for accelerating returns; without a sufficient number of competitors, that potential is not realized as disruptive selection.

The I-Condition is generated by a pure Payoff (Regulation) module. Stabilizing feedback arises from interference competition, as the term  $(N-1)b(y)$  in the denominator ensures that a strategy's payoff decreases as it becomes more common.

This deconstruction reveals that the number of competitors,  $N$ , acts as a pleiotropic regulating factor. It is a crucial parameter in the modules that establish all three conditions ( $S$ ,  $H$ , and  $I$ ), making the Contest Model a deeply coupled system. The framework's value lies in its ability to parse this complexity and reveal the distinct causal contribution of each component to the final evolutionary outcome.



## 6. Scenario Assembly and Design Space

---

Using the library begins with selecting modules whose primary functions match the evolutionary effects you want to include. These can act independently or in coupled form, where the same mechanism influences more than one condition. Coupling is common in real systems and should be identified early, since it can change the outcome of later stability checks.

Once the modules are chosen, they are combined into an explicit invasion fitness function  $p(x, y)$ . From this, you calculate the local fitness derivatives  $S$ ,  $H$ , and  $I$  at the candidate singular strategy  $x^*$ . This provides the first filter:  $S=0$ ,  $H>0$ , and  $I<0$  must hold.

The next steps follow the stability pipeline from the parent framework. Check convergence stability by verifying that the slope of  $S$  at  $x^*$  is negative. Test hyperbolic stability by ensuring the Jacobian of the full oligomorphic dynamics is nonsingular at the equilibrium. Confirm qualitative dissimilarity, meaning the coexisting morphs differ enough in ecological effect to avoid collapse.

Only when a scenario passes all these steps can it be considered a plausible, stable adaptive polymorphism. This process turns the module library into a systematic tool for exploring both known and novel parts of the design space while staying grounded in the theoretical foundations of the parent model.

## 7. Example Scenarios

---

The scenarios below are presented as conceptual sketches rather than complete analytical models. Their purpose is to show how the modular framework can be applied in different configurations, from single-slot designs to coupled multi-slot architectures.

### 7.1. Single-slot scenario: classic trade-off equilibrium

Modules: Phenotype (Production) →  $S=0$ , Payoff (Production) →  $H>0$ , Fitness (Regulation) →  $I<0$ .

Concept: A plant invests in root vs shoot growth, creating a trade-off ( $S=0$ ). Increased investment in roots gives diminishing returns, creating curvature ( $H>0$ ). Competition for light among individuals creates stabilising frequency dependence ( $I<0$ ).

Point to highlight: Shows how independent modules fill the three slots without coupling.

### 7.2. Coupled scenario: contest model variant

Modules: Mixed (Payoff) →  $S$ ,  $H$ , and  $I$  all affected.

Concept: A contest for a resource where individual investment affects both own payoff and competitor's payoff, generating the equilibrium ( $S$ ), curvature ( $H>0$  from accelerating returns), and stabilising feedback ( $I<0$  from competitive interference).

Point to highlight: All three conditions come from the same coupled mechanism; must check for stability carefully.

## 8. Conclusion and Implications

---

This modular approach is a hypothesis-generation and model-design tool that operates within the production-regulation decomposition of my primary framework. By making each branching condition an explicit “slot” with interchangeable biological mechanisms, it facilitates the systematic exploration of adaptive polymorphism scenarios.

The framework’s most significant implication is its power as a hypothesis-generation engine. Instead of only analyzing existing models, we can now systematically construct new, plausible biological scenarios. Furthermore, by providing a common language, it allows models from different theoretical traditions to be analyzed through the same functional lens, revealing deep structural similarities between them and contributing to a unified synthesis.

Ultimately, this approach provides the tools to map the full design space of adaptive polymorphism and to classify the architectural patterns of the models themselves. We can distinguish between Pure Decoupled Systems, where each condition is met by an independent module, Hybrid/Mixed Systems, where a condition is met by an inseparable mix of production and regulation, and Coupled Systems, where a single module has pleiotropic effects on multiple conditions. Recognizing these patterns is the final step in deconstructing the full causal architecture of any evolutionary scenario.

# Reciprocal Negative Feedbacks Stabilize an Emergent Polymorphism in a Cross-Feeding Microbial Consortium

---

## 1. Introduction

---

*Pseudomonas putida* presents a well-defined biological problem, as this diversity is conditional on a cross-feeding interaction with a partner species, *Acinetobacter johnsonii* (Al-Tameemi and Rodríguez-Verdugo, 2024). To formally dissect this problem, we apply the theoretical framework of Lehmann and Mullon, 2025 using a modular approach. This deconstructs any stable adaptive polymorphism into three necessary functional components: a trade-off (S-Condition), disruptive selection (H-Condition), and stabilizing feedback (I-Condition).

Two of these components are well-explained by established mechanisms in this system. The S-Condition (the trade-off) is established by a Phenotype level Production module, where a single, large-effect mutation in the *fleQ* gene creates an intrinsic resource allocation trade-off between motility and metabolic uptake efficiency, giving rise to the high-yield harvester morph (Al-Tameemi and Rodríguez-Verdugo, 2024). The H-Condition (disruptive selection) is generated by a Phenotype level Regulation module. The partner species, *A. johnsonii*, acts as a niche constructor by creating a heterogeneous landscape of benzoate patches, which favors the distinct specialist strategies of the forager and harvester while selecting against intermediates (Christensen et al., 2002; Hansen et al., 2007). This deconstruction reveals that the I-Condition (stabilizing feedback) is the core of the unresolved puzzle. Reciprocal invasion assays in well-mixed liquid cultures failed to detect the negative frequency-dependent selection required for coexistence, explicitly ruling out a simple, spatially-independent mechanism (Al-Tameemi and Rodríguez-Verdugo, 2024). The framework thus guides the formulation of three distinct, spatially-explicit hypotheses for this unknown stabilizing mechanism.

### 1.1. Hypothesis 1: Stabilization via Indirect Reciprocal Negative Feedback

The stabilizing feedback ( $I < 0$ ) required for coexistence is hypothesized to be an emergent property of two distinct, reciprocal negative interactions between the morphs, each corresponding to a different regulatory module from the theoretical framework.

First, the motile forager population acts through a Phenotype level Regulation ( $e_z$ ) module. By globally depleting the primary resource, foragers impose a negative, frequency-dependent fitness cost on the sessile harvesters, which depend on high local resource concentrations (Christensen et al., 2002).

Conversely, the harvester population acts through a Fitness level Regulation ( $e_p$ ) module. Through localized, high-density metabolism, harvesters create anoxic microenvironments, imposing a dynamic of competitive "suffocation" that is inhibitory to the motile foragers (Xavier and Foster, 2007).

Together, these independent regulatory modules are predicted to create the reciprocal negative feedback loop necessary to stabilize the polymorphism. As one morph becomes more common, it disproportionately harms the other, preventing competitive exclusion.

## 1.2. Hypothesis 2: Stabilization via Hybrid Niche Construction

The stabilizing feedback ( $I < 0$ ) is hypothesized to emerge from a Hybrid/Mixed Module, where coexistence is an emergent property of niche construction by the harvester morph and a trait-mediated response by the forager morph.

The mechanism unfolds in three steps. First, dense harvester clusters construct an anoxic micro-niche through their collective metabolism, which acts as the primary regulating factor  $e_p$ . Second, the forager's ancestral production factor  $z$  is its programmed "oxygen-starvation dispersal response", which causes it to be actively expelled from these anoxic zones. Finally, the harvester morph, having lost this ancestral response due to mutations affecting motility and surface properties such as *fleQ* or *wapH*, can tolerate and persist within the very niche it creates.

This interaction generates stabilizing feedback by creating a protected spatial refuge for the harvesters. The forager's own phenotype leads to its self-exclusion from harvester-dominated territory, shielding the harvesters from direct competition. Furthermore, this mechanism is predicted to have a secondary, reinforcing effect on disruptive selection ( $H > 0$ ). By hardening the boundaries between the anoxic harvester niche and the oxic forager niche, it further penalizes intermediate strategies, thus strengthening the fitness valley that favors the two specialized morphs.

## 1.3. Hypothesis 3: Stabilization via Coupled Niche Construction and Pleiotropy

We hypothesize that the polymorphism is maintained by a Coupled Module, where disruptive selection ( $H > 0$ ) and stabilizing feedback ( $I < 0$ ) are the pleiotropic effects of a single biological process: the formation of dense biofilms by the harvester morph. This process is driven by the *fleQ* master regulator, which inversely controls motility and the production of biofilm matrix components. The pleiotropic nature of this regulator is predicted to satisfy two distinct conditions for adaptive polymorphism simultaneously:

**Disruptive Selection ( $H > 0$ ):** The formation of a physically distinct biofilm constitutes niche construction. This acts as a Phenotype (Regulation)  $e_z$  module, creating a spatially heterogeneous landscape. It generates strong disruptive selection by favoring the high-yield harvester strategy within the biofilm niche and the motile forager strategy outside of it, while selecting against intermediate phenotypes.

**Stabilizing Feedback ( $I < 0$ ):** Concurrently, the same biofilm structure provides stabilizing feedback. The high cell density and matrix create localized anoxic zones that inhibit the oxygen-sensitive foragers. This acts as a Payoff (Regulation)  $e_\pi$  module, where interference from the harvester's constructed niche reduces the forager's ability to grow and compete, thus preventing the forager from invading. In this scenario, a single pleiotropic genetic switch (*fleQ*) drives one process (biofilm formation) that generates both disruptive and stabilizing forces. This hypothesis is consistent with the experimental observation that the polymorphism is only maintained in a spatially structured context.

## 2. Aim

---

To begin dissecting these possibilities, the present study develops a computational model to formally test the first and most parsimonious of these hypotheses: Indirect Reciprocal Negative Feedback. This initial model is designed to evaluate whether the stable polymorphism can be explained solely by foundational ecological interactions global resource depletion by one morph and localized niche construction (anoxia) by the other. By establishing a baseline model for this core mechanism, we can determine the sufficiency of these simple feedbacks in maintaining coexistence. The latter two hypotheses, which invoke more complex trait-mediated behaviors and biofilm dynamics, are therefore presented as distinct, plausible alternatives whose investigation would require future, specialized models.

## 3. Methods: An Agent-Based Model of Polymorphism

---

### 3.1. Model Rationale and Focus

A key feature of this model is its starting point with two discrete, coexisting morphotypes, the motile "forager" and the non-motile "harvester." This design choice is a direct reflection of the specific biological system under investigation and represents a departure from classic adaptive dynamics models, which typically analyze the gradual emergence of polymorphism from a single ancestral lineage (Lehmann and Mullon, 2025). The *Pseudomonas putida* system provides a biological "shortcut" to this process; the experimental literature demonstrates that a single, large-effect mutation in the *fleQ* gene is sufficient to create the non-motile, high-yield "harvester" morph from the ancestral "forager" type (Al-Tameemi and Rodríguez-Verdugo, 2024). Consequently, our model is not designed to investigate the origin of this polymorphism (the S and H conditions) but to focus entirely on the ecological conditions required for its stable maintenance, which is governed by the stabilizing feedback of the I-condition  $I < 0$ .

Because the experimental literature indicates this stabilizing mechanism is spatially dependent and is not detectable in well-mixed cultures (Al-Tameemi and Rodríguez-Verdugo, 2024), a two dimensional, spatially explicit agent based model (ABM) was constructed. The model simulates the growth, movement, and interaction of individual "Forager" and "Harvester" morphotypes of *P. putida* competing for diffusing benzoate and oxygen. The environment is shaped by the partner species, *Acinetobacter johnsonii*, which is abstracted in the model as the fixed, benzoate-producing source points (Christensen et al., 2002; Hansen et al., 2007).

#### 3.1.1. Model Environment

The simulation environment consists of a  $100 \times 100$  grid with periodic boundary conditions. Benzoate is produced at a constant rate,  $p_{bzn}$ , from a fixed lattice of source points. Oxygen is supplied uniformly across the grid at a constant influx rate,  $p_{O_2}$ . Both substrates are subject to diffusion and a uniform washout rate,  $w$ . Diffusion is modeled at each time step using a 2D convolution with a five-point Laplacian kernel, governed by diffusion coefficients  $D_{bzn}$  for benzoate and  $D_{O_2}$  for oxygen.

### 3.1.2. Agent Behaviors

Each agent is characterized by its spatial position and biomass. The model progresses in discrete time steps, during which the following agent behaviors are executed in sequence:

**Substrate Uptake:** A decoupled uptake mechanism was implemented. The potential uptake rate,  $U$ , for each substrate was calculated for each agent based on local substrate concentration  $[S]$  using Michaelis-Menten kinetics:

$$U = V_{max} \frac{[S]}{K_m + [S]}.$$

Scenario-specific efficiency multipliers,  $\mu_{bzn}$  for foragers and  $\mu_{O2}$  for harvesters, were applied to the potential uptake rates. The growth of an agent is determined by the single limiting substrate,

$$U_{lim} = \min(U_{bzn}, U_{O2}).$$

However, the amount of each substrate removed from the environment is based on its full potential uptake rate ( $U_{bzn}$  and  $U_{O2}$ ), simulating wasteful consumption. For harvesters, oxygen consumption is distributed over a  $3 \times 3$  grid cell area centered on the agent.

**Growth and Death:** The biomass of each agent,  $B$ , is updated based on the limiting uptake rate, substrate-specific yield coefficients  $Y_f$  for foragers,  $Y_h$  for harvesters), and maintenance costs  $c_{maint}$  for both  $c_{motility}$  for foragers only). The change in biomass is calculated as

$$\Delta B = (U_{lim} \cdot Y) - c_{maint} - c_{motility}.$$

Agents with a biomass of zero or less are removed from the simulation.

**Division:** Agents with a biomass greater than or equal to two undergo division. The parent agent's biomass is reset to one, and a new daughter agent with a biomass of one is placed in a randomly selected adjacent grid cell. A global population limit,  $N_{max}$  is enforced.

**Movement:** Foragers exhibit a "smart flee" dispersal behavior. If the local oxygen concentration falls below a defined threshold,  $\theta_{O2}$  the agent relocates to a randomly selected grid cell where the oxygen concentration is above this threshold. If no such sites are sufficiently available, it relocates to a random position on the grid. In oxygen-sufficient conditions, foragers perform a random walk to an adjacent cell. Harvesters are non-motile.

All simulations were initiated with 50 forager and 50 harvester agents, each with a biomass of 1.0, placed at random positions on the grid. Resource grids were initially set to zero.

Model parameters, listed in full in Supplementary Table 1, were selected and calibrated to ensure stable coexistence in the control scenario, consistent with the dynamics observed in the experimental system.

## 4. Results

### 4.1. Competitive Balance is Sensitive to Specialist Efficiency

To establish the baseline competitive dynamics of the system, we first simulated three scenarios in which the metabolic efficiencies of the specialists were altered. Under the control parameters, the model produced a stable coexistence between the two morphs, characterized by harvesters forming dense clusters at resource source points and foragers occupying the periphery (Fig. 1A-B). This balance, however, was sensitive to the strength of the trade-off. A significant increase in the harvester's oxygen uptake efficiency led to the competitive exclusion of the forager (Fig. 1C-D). Conversely, a large increase in the forager's benzoate uptake efficiency resulted in the collapse of the harvester population (Fig. 1E-F). These results confirm that a balanced trade-off is required for coexistence and motivate a direct test of the underlying stabilizing mechanism.

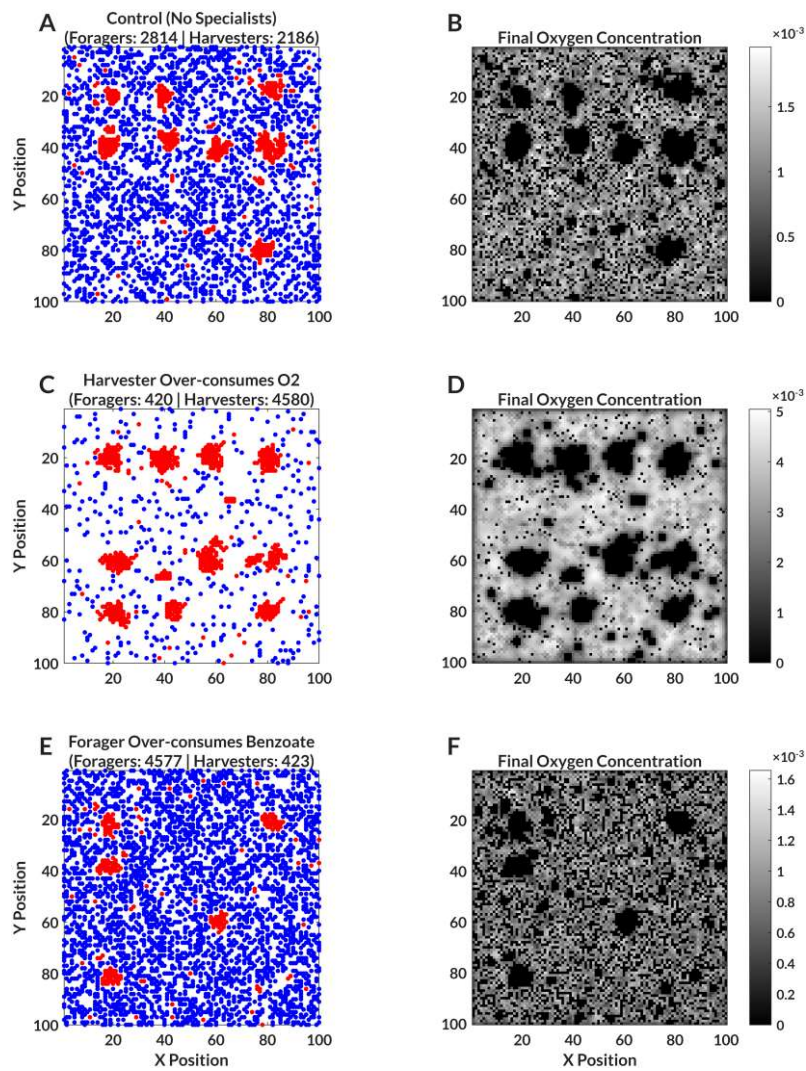


**Figure 1 | Effect of Specialist Strategies on Community Structure and Environment.**

Final states from the agent-based model comparing three metabolic scenarios. Left panels (A, C, E) show the final spatial distribution of Forager (blue) and Harvester (red) agents. Right panels (B, D, F) show the corresponding final oxygen concentration grid, where white indicates high concentration. Scenarios are: **(A-B)** Control ( $\mu_{bzn} = 1.0$   $\mu_{O_2} = 2.5$ ); **(C-D)** Harvester Specialist ( $\mu_{O_2} = 10.0$ ); and **(E-F)** Forager Specialist ( $\mu_{bzn} = 15.0$ ).

## 4.2. In Silico Invasion Analysis Reveals Stabilizing Feedback

To formally test for the presence of the stabilizing feedback ( $I < 0$ ) proposed in Hypothesis 1, we performed an *in silico* invasion analysis. The analysis revealed a strong negative correlation between the initial frequency of the forager morph and its relative fitness (Fig. 2). The forager exhibited a positive selection rate when rare, indicating it could successfully invade a resident population of harvesters. As the forager's frequency increased, its relative fitness declined, becoming negative when it was the common type. The negative slope of the linear regression, which intersects the equal fitness line, is the definitive signature of negative frequency-dependent selection. This result demonstrates that the reciprocal negative feedbacks implemented in our spatial model are sufficient to generate the stabilizing mechanism required for stable coexistence.

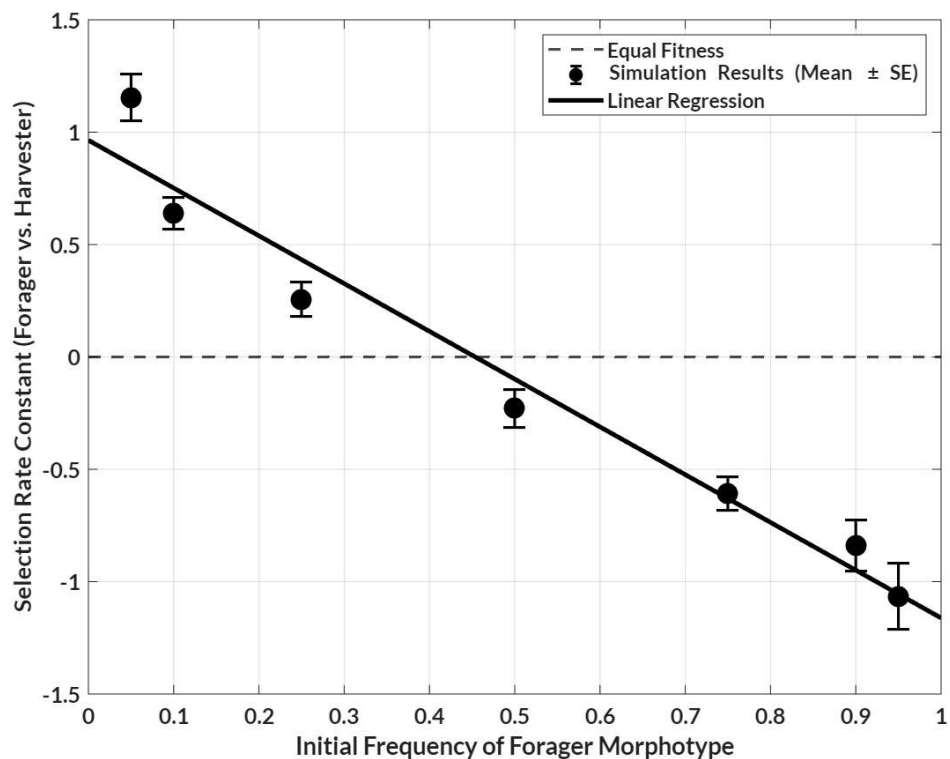


**Figure 2 | In Silico Invasion Analysis Demonstrates Negative Frequency-Dependent Selection.**

The relative fitness of the forager morph (selection rate constant, y-axis) is plotted as a function of its initial frequency in the population (x-axis). A positive selection rate indicates a fitness advantage for the forager. Each point represents the mean of 10 replicate agent-based simulations ( $\pm$ SE). The solid line shows the linear regression of the data, and the dashed line indicates equal fitness between the two morphs. The negative slope, which crosses the equal fitness line, is the definitive signature of negative frequency-dependent selection that allows for stable coexistence.

## 5. Discussion

---

Our agent-based model demonstrates that the reciprocal negative feedback proposed in Hypothesis 1 are a sufficient mechanism to explain the stable coexistence of the forager and harvester morphs of *P. putida*. The *in silico* invasion analysis successfully reproduced the negative frequency-dependent selection required for a stable polymorphism. This is a critical result, as this stabilizing feedback was absent in previous well-mixed experimental assays. This finding suggests that simple, foundational ecological interactions, when expressed in a spatially explicit context, can generate the necessary conditions for maintaining an adaptive polymorphism as described by our theoretical framework.

A point of theoretical precision is warranted here. While our model's demonstration of negative frequency-dependent selection (Fig. 2) is the definitive signature of a stable coexistence, it is imprecise to label this outcome itself as  $I < 0$ . The selection interaction coefficient,  $I(x^*) = \frac{\partial^2 p}{\partial x \partial y} |_{x=y=x^*}$ , is a specific, local property of the fitness function evaluated at the monomorphic singular strategy from which branching originates. Our model, by starting with two established morphotypes, does not simulate this branching event but rather the subsequent ecological dynamics. The result in Figure 2 is therefore more accurately described as a demonstration of system-level negative frequency-dependent selection. This selection is the consequence of such stabilizing forces, not a direct measurement of the local coefficient  $I$  itself.

Our model offers a resolution to the central puzzle motivating this work, which was the observation of a stable polymorphism conditional on the presence of *A. johnsonii* that could not be explained by simple frequency-dependence. The model shows how spatial structure is the key by synthesizing two independently observed phenomena into a single, cohesive mechanism. The global benzoate depletion by motile foragers, which harms sessile harvesters, is a known dynamic in biofilms, while the localized anoxia created by dense cell clusters, which harms motile foragers, has also been experimentally demonstrated.

While this model provides a robust, proof-of-concept explanation, it is important to acknowledge its simplifying assumptions. The partner species, *Acinetobacter johnsonii*, was abstracted as a static environmental feature rather than a dynamic population, and the simulation is two-dimensional, whereas real biofilms have complex three-dimensional structures. Furthermore, our model's support for Hypothesis 1 does not preclude the action of the alternative mechanisms proposed in Hypotheses 2 and 3. These limitations highlight clear avenues for future research. The model makes testable predictions, such that future experimental work could quantify the predicted resource gradients in co-culture or could be designed to decouple the feedback loops, for instance, by negating the effects of anoxia in a hyperoxic environment. Future computational studies should also expand upon this model to explicitly test Hypotheses 2 and 3.

In conclusion, this study provides a plausible and mechanistic resolution to a key puzzle in experimental evolution. More broadly, our work underscores the critical role of spatial structure and reciprocal niche construction in maintaining microbial diversity. It demonstrates how simple, local interactions can generate the complex, system-level feedbacks required to stabilize polymorphisms that arise from single, large-effect mutations. This provides a key insight into how the vast functional diversity observed in natural microbial communities can be maintained.

## 6. Supplementary Info

---

Supplementary Table 1 | Core Model Parameters

Parameter	Symbol	Description	Value
Agent Properties			
Forager Yield	$Y_f$	Biomass produced per unit of resource consumed by a forager.	0.50
Harvester Yield	$Y_h$	Biomass produced per unit of resource consumed by a harvester.	0.55
Motility Cost	$c_{motility}$	Biomass cost per time step for forager movement.	1e-4
Maintenance Cost	$c_{maint}$	General biomass cost per time step for all agents.	1e-4
Resource Dynamics			
Benzoate Diffusion	$D_{bzn}$	The diffusion coefficient for benzoate across the grid.	0.1
Oxygen Diffusion	$D_{O_2}$	The diffusion coefficient for oxygen across the grid.	0.2
Benzoate Production	$p_{bzn}$	Rate of benzoate production at source points per time step.	3.0
Oxygen Influx	$p_{O_2}$	Rate of uniform oxygen influx across the grid per time step.	4e-4
Washout Rate	$w$	Proportion of all resources removed from the grid per time step.	5e-2
Uptake Kinetics			
Max Uptake Rate	$V_{max}$	The maximum potential substrate uptake rate (unmodified).	1.0
Oxygen Half-Saturation	$K_{m,O_2}$	Oxygen concentration at which uptake is half of $V_{max}$	1e-2
Benzoate Half-Saturation	$K_{m,bzn}$	Benzoate concentration at which uptake is half of $V_{max}$	1e-2
Forager Benzoate Multiplier	$\mu_{bzn}$	Uptake efficiency multiplier	1.0

		for benzoate, specific to foragers.	
Harvester O <sub>2</sub> Multiplier	$\mu_{O_2}$	Uptake efficiency multiplier for oxygen, specific to harvesters.	2.5
<b>Behavior &amp; Simulation</b>			
Oxygen Flee Threshold	$\theta_{O_2}$	Oxygen concentration below which foragers initiate dispersal.	5e-4
Max Population	$N_{max}$	The maximum number of agents allowed in the simulation.	5000
Grid Size	-	The dimensions of the square simulation grid.	100x100
Simulation Duration	-	The maximum number of time steps for each simulation run.	1500

## 7. References

---

1. Al-Tameemi, Z. and Rodríguez-Verdugo, A. (2024) 'Microbial diversification is maintained in an experimentally evolved synthetic community', *mSystems*. Edited by W.R. Harcombe, 9(11), pp. e01053-24. Available at: <https://doi.org/10.1128/msystems.01053-24>.
2. Christensen, B.B. et al. (2002) 'Metabolic Commensalism and Competition in a Two-Species Microbial Consortium', *Applied and Environmental Microbiology*, 68(5), pp. 2495–2502. Available at: <https://doi.org/10.1128/AEM.68.5.2495-2502.2002>.
3. Hansen, S.K. et al. (2007) 'Evolution of species interactions in a biofilm community', *Nature*, 445(7127), pp. 533–536. Available at: <https://doi.org/10.1038/nature05514>.
4. Lehmann, L. and Mullon, C. (2025) 'Evolution of quantitative traits: exploring the ecological, social and genetic bases of adaptive polymorphism'. *bioRxiv*, p. 2025.06.23.661088. Available at: <https://doi.org/10.1101/2025.06.23.661088>.
5. Xavier, J.B. and Foster, K.R. (2007) 'Cooperation and conflict in microbial biofilms', *Proceedings of the National Academy of Sciences*, 104(3), pp. 876–881. Available at: <https://doi.org/10.1073/pnas.0607651104>.